

# Arc-Fault Detector Algorithm Evaluation Method Utilizing Prerecorded Arcing Signatures

Jay Johnson<sup>1</sup> and Jack Kang<sup>2</sup>

<sup>1</sup>Sandia National Laboratories, Albuquerque, NM, USA

<sup>2</sup>Sensata Technologies, Attleboro, MA, USA

## ABSTRACT

*Abstract* — The 2011 *National Electrical Code*® Article 690.11 requires photovoltaic systems on or penetrating a building to include a DC arc-fault protection device. In order to satisfy this requirement, new Arc-Fault Detectors (AFDs) are being developed by multiple manufacturers including Sensata Technologies. Arc-fault detection algorithms often utilize the AC noise on the PV string to determine when arcing conditions exist in the DC system. In order to accelerate the development and testing of Sensata Technologies' arc-fault detection algorithm, Sandia National Laboratories (SNL) provided a number of data sets. These prerecorded 10 MHz baseline and arc-fault data sets included different inverter and arc-fault noise signatures. Sensata Technologies created a data evaluation method focused on regeneration of the prerecorded arcing and baseline test data with an arbitrary function generator, thereby reducing AFD development time.

*Index Terms* — photovoltaic systems, arc-fault detection, series arc-faults, monitoring, power system safety

## I. INTRODUCTION

In order to improve fire safety in PV systems, the 2011 *National Electrical Code*® (NEC) [1] requires series arc-fault protection. Arc-fault circuit interrupters (AFCI) meet this requirement by containing an arc-fault detector (AFD), which identifies the arc-fault, and a circuit interrupter, which de-energizes the PV system. In order to create robust arc-fault detection algorithms tests must be completed on a range of PV systems: the algorithm must not nuisance trip on different inverter noise signatures, while also detecting arcing within the times prescribed in UL 1699B [2].

In order to accelerate robust algorithm development, Sandia National Laboratories collected noise signatures from different arc-faults and inverters. These files have been provided to Sensata Technologies to test their AFD hardware by recreating baseline and arc-fault current signatures. The advantage of this method over traditional AFD development is that the AFD algorithm can be tuned quickly, does not require access to PV field sites, avoids the hazards associated with generating arcs, and can be completed in a laboratory environment which is unaffected by weather.

Previously Sensata pursued multiple software tools to simulate PV string current during arcing phenomena. Models were built in Matlab, LTSPICE, and Excel to simulate the arc and the detection algorithm. However the software simulations were limited to reduced-order models which did not incorporate all the physical aspects of the PV system hardware or arcing dynamics. In this paper we proposed a new method based on an arbitrary function generator to simulate arc-fault noise in order to develop better arc-fault detection tools. The main objective of this work is to present a PV arc-fault detector evaluation method based on an arbitrary function generator which recreates the inverter noise and arc waveforms obtained from previous PV arc-fault tests. The purpose is to feed the waveforms to an AFD device to help tune AFD hardware and software parameters.

## II. DEVELOPMENT OF SIGNATURE LIBRARY

### A. Resistance to Inverter Nuisance Tripping

Sandia National Laboratories (SNL) is collecting high data rate current signatures of a number of PV systems to better characterize the range of inverter noise. Inverter noise varies greatly between manufacturer and model. The magnitude and excited frequencies drastically differ between inverters due to differences in transistor switching noise, galvanic coupling from the AC side of the array to the DC (especially for transformerless inverters), and maximum power point tracking (MPPT) algorithm behavior. Furthermore, charge controllers, DC/DC converters, and microinverters each have different switching behaviors. All these differences are difficult to account for while designing arc-fault detector algorithms because of time constraints, limited development budgets, and difficulty accessing a wide-range of equipment.

The Distributed Energy Technologies Laboratory at SNL has approximately 150 kW of PV with a range of inverters, converters, and charge controllers for testing and evaluating PV prototypes and grid interactions. The diverse collection of inverters was used to populate a library of different baseline or non-arcing signatures that were used to test for

AFD nuisance tripping. Different noise signatures from residential-scale inverters in the frequency domain are shown in Fig. 1. These were collected with a Tektronix TCP303 connected to National Instruments PXI-5922 digitizer. The Fast Fourier Transform was performed with a Hanning window on 262,144 ( $2^{18}$ ) DC current data samples captured at 10 MHz.

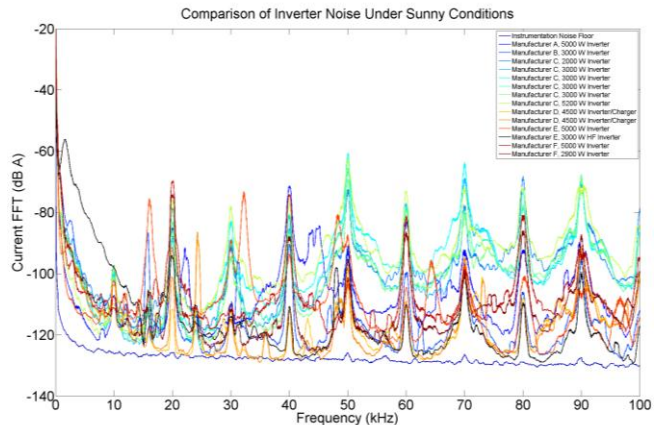


Fig. 1. Different inverter noise signatures smoothed with an 800 Hz sliding-window.

In order to determine the number of signatures that must be captured for a single inverter model, four identical inverters were measured for the DC noise signature. It was determined that the same inverter models produce similar switching noise for identical arrays and meteorological conditions, shown in Fig. 2. Although, there can be additional sources of noise from RF or galvanic coupling, as shown by the elevated noise content in one of the black traces in Fig. 2. The source of this additional noise is unknown, but it is possible that it could trip an AFD, so careful selection of the AFD algorithm is critical.

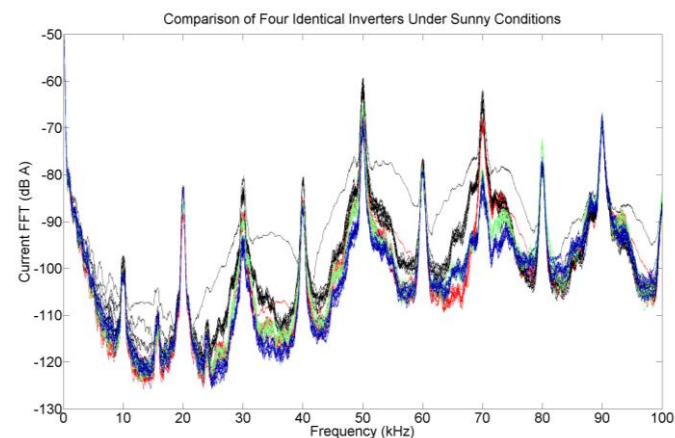


Fig. 2. 10 noise signatures for four identical 3000 W inverters (red, blue, green, black), smoothed with an 800 Hz sliding-window.

Inverters do not behave the same way for all irradiance conditions. In the morning and evening, inverters turn on and off—often repeatedly—while trying to generate power for the longest period of time possible. This process is shown in Fig. 3 for the morning. During this period as well as during cloudy conditions, inverter noise signatures change. An example of the change is shown in Fig. 4 for two sets of 10 consecutive recordings taken 5 minutes apart during a partly cloudy day with plane of array irradiances of  $\sim 1130$  and  $\sim 300$   $\text{W}/\text{m}^2$ . The 5000 W inverter increases the noise around 23 and 46 kHz when a cloud comes over the array. Due to the change in noise, it is important to test AFDs for multiple irradiance conditions, and therefore it was necessary to capture noise signatures from inverters at different irradiance levels for the SNL arc-fault library as well. SNL is capturing inverter signatures at three global horizontal irradiances:  $< 300$   $\text{W}/\text{m}^2$ ,  $\sim 500$   $\text{W}/\text{m}^2$ , and  $> 900$   $\text{W}/\text{m}^2$ .

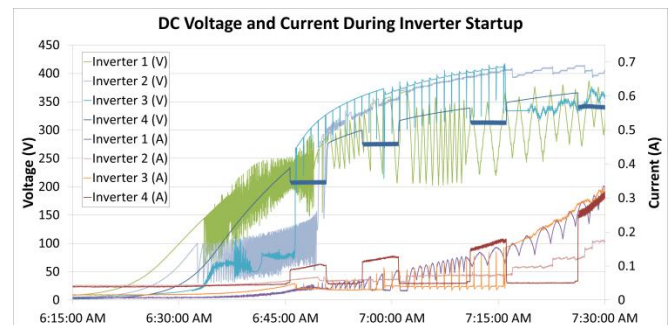


Fig. 3. DC voltage and current for four different inverters during morning startup at DETL. During this period—as well as during different irradiance levels—the inverter will produce different noise signatures.

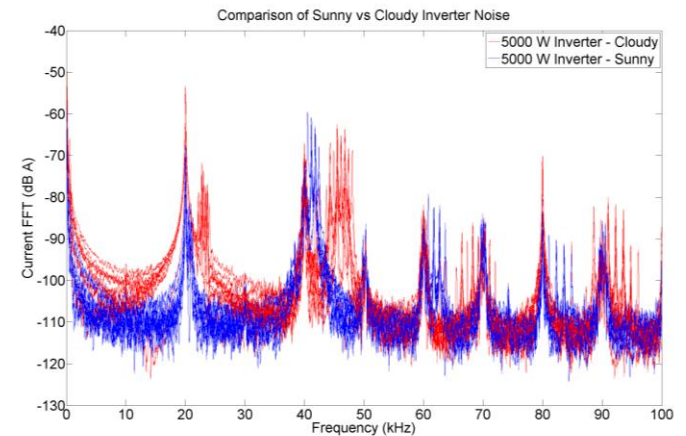


Fig. 4. Inverter noise signatures for sunny ( $\text{POA} = 1130$   $\text{W}/\text{m}^2$ ,  $4250$   $\text{W}_{\text{DC}}$ ) and cloudy ( $\text{POA} = 300$   $\text{W}/\text{m}^2$ ,  $1200$   $\text{W}_{\text{DC}}$ ) conditions, smoothed with a 160 Hz sliding-window.

### B. Arc-fault Noise Signatures

There has been significant work at Sandia National Laboratories generating and characterizing different arc-faults [3-5]. During this process hundreds of series and parallel arc-fault signatures have been captured on multiple

arrays. Some of these signatures are being cataloged for future reference. An example of arcing noise and baseline inverter noise is shown in Fig. 5.

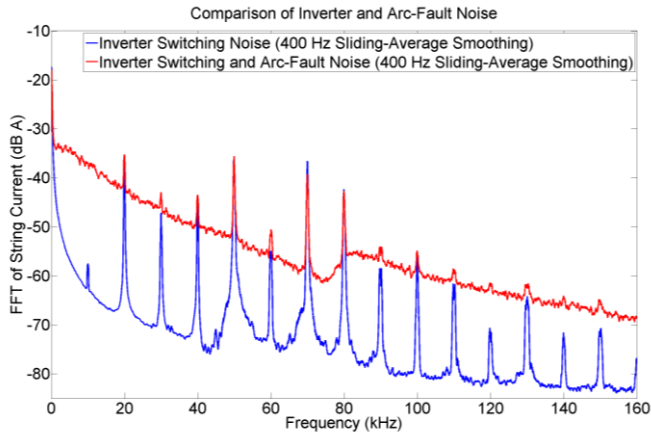


Fig. 5. Inverter and series arc-fault noise comparison.

### III. ARC-FAULT DETECTOR EVALUATION

#### A. Test Setup and AFD Algorithm Evaluation Method

In order to recreate the SNL current baseline and arc-fault recordings, Sensata Technologies used a 30 MHz Agilent 33522A Arbitrary Waveform Generator with 16 MSA expansion memory. The function generator played back the 10 MHz data sets at 10 MS/s speed and the signal was routed to the current transformer (CT) on the prototype arc-fault detector. Trip times and other AFD outputs from the test were displayed on a DPO4034B oscilloscope. The test setup is shown in Fig. 6.

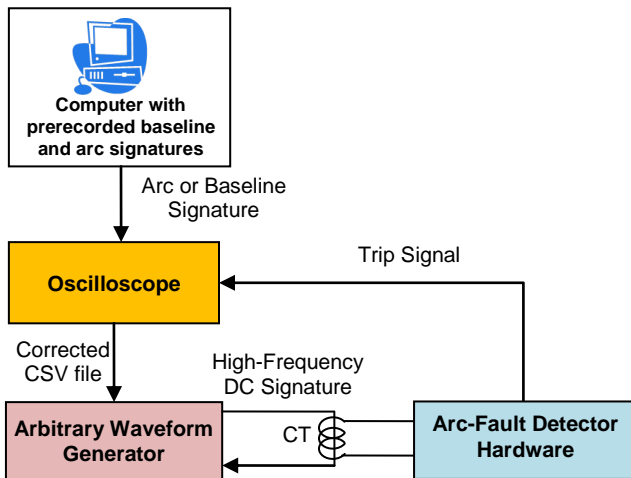


Fig. 6. Experimental test setup with arbitrary waveform generator and prototype arc-fault detector.

Sensata Technologies developed the following procedure for evaluating the AFD:

1. Import the arc-fault or baseline signature into the oscilloscope.
2. Save the oscilloscope trace to a .csv file.
3. If necessary, correct the errors in the .csv file, by replacing non-numerical characters (e.g., “inf”) with previous data point.
4. Export the .csv file into the function generator.
5. Monitor arc-fault detector for correct response to given input.

#### B. Testing

A series of tests were performed with the data provided by SNL. The signatures were similar to the data collected in previous tests [3], and included:

1. Multiple arcing and non-arcing signatures from a 1.2 kW crystalline Si string with a load bank and an inverter.
2. Arcing and non-arcing data for three different Si strings connected to the same 3-phase inverter.
3. Baseline inverter noise signatures from six different inverters.
4. Noise from opening and closing a combiner box DC disconnect.

Arcing signatures were generated to demonstrate the AFD could successfully identify arc-faults. Inverter noise signatures and DC disconnect signatures were replayed to ensure the arc-fault detector did not nuisance trip on these events.

Fig. 7 shows the current signature from an arc-fault data set in the oscilloscope. This time-history is replayed by the arbitrary waveform generator. Fig. 8 shows four current transformer (CT) measurements of the AC current content of arc-faults in the field. The Sensata Technologies device monitors the AC current signal and detects the elevated AC content. Using this technique the arc-fault can be identified and de-energized.

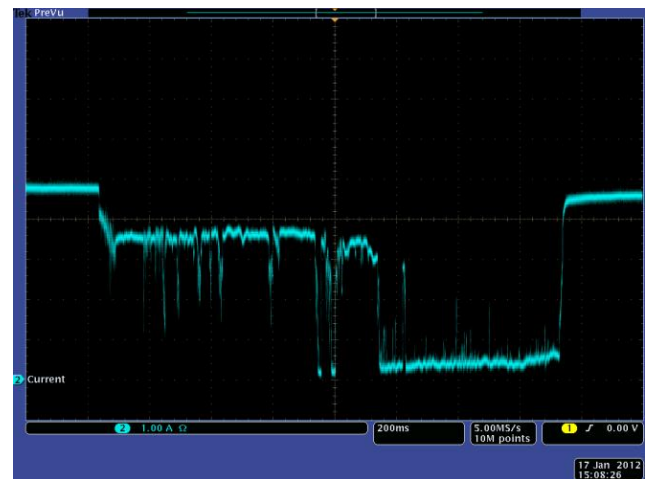


Fig. 7. DC arc-fault current waveform from a “typical” arc-fault generated on a single PV string.

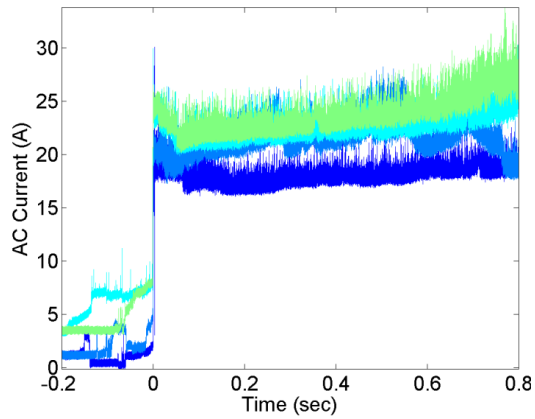


Fig. 8. Multiple recorded series arc-fault AC current waveforms measured with a current transformer.

The Sensata Technologies AFD measures the current transformer secondary voltage for arc-fault detection. The current transformer secondary voltage is calculated by

$$V_s = M \frac{di_p}{dt} \quad (1)$$

where  $V_s$  is the secondary voltage,  $i_p$  is the primary current, and  $M$  is the mutual inductance. The ratio between measured primary current and secondary voltage output was 20 A:1.2 V. Knowledge of this ratio was used to tune the arc-fault detector circuit parameters based on results from the replayed baseline and arc-fault current signatures.

### C. AFD Evaluation Case 1: Arcing Current

In order to evaluate the arc-fault detection algorithm, the arcing signatures, like those in Fig. 7, were replayed into the Sensata Technologies AFD. In Fig. 9, the dark blue trace was selected to be regenerated by the function generator. The yellow trace shows the derivative of the current with respect to time as well as the trip signal. The trip time for this test was ~400 ms.

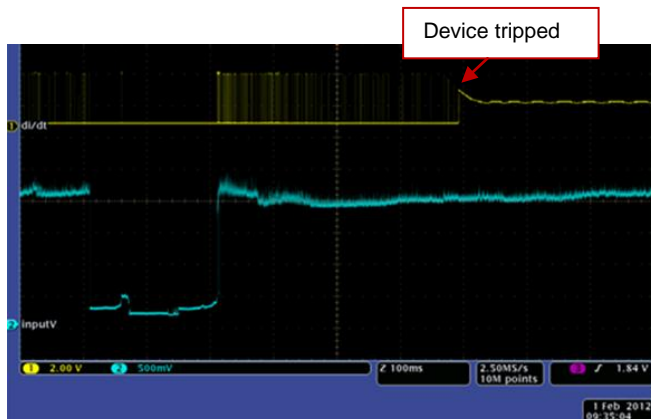


Fig. 9. Function generator and AFD output displayed on the oscilloscope.

### D. Waveform Evaluation Case 2: Pulse Data

Sensata Technologies was able to further refine their arc-fault detection algorithm using known relationships between the arcing signature and the AFD circuitry. In the AFD a current ‘pulse’ is created by the frontend analog circuits by the AC arc-fault current component after high-pass filtering. This pulse was fed into the AFD circuit to better tune the arc-fault detector. Figure 4 shows the string current (Hall Effect), the arc-fault voltage (Arc V (TEK)), and the arcing current AC component (Pearson) for an arc-fault signature along with the arcing current pulse generated from the AFD front end circuits.

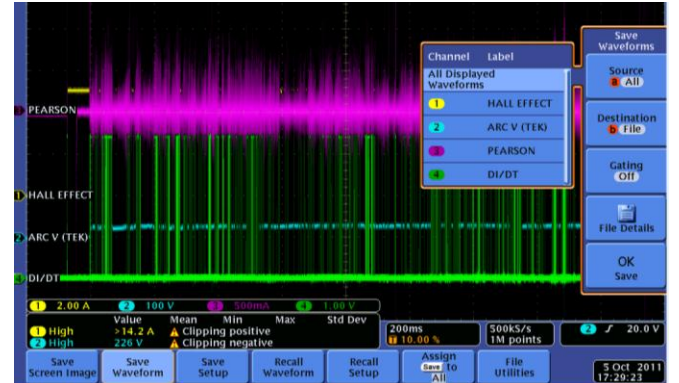


Fig. 10. Function generator and AFD output. The green trace is selected to be regenerated by the function generator to help tune the software algorithm.

The measured arcing current pulse waveform was regenerated by the function generator and applied to the AFD device analog circuits. The result shows the device tripped in less than 1 second, shown in Fig. 11. This method was effectively used to tune the Sensata Technologies software algorithm.

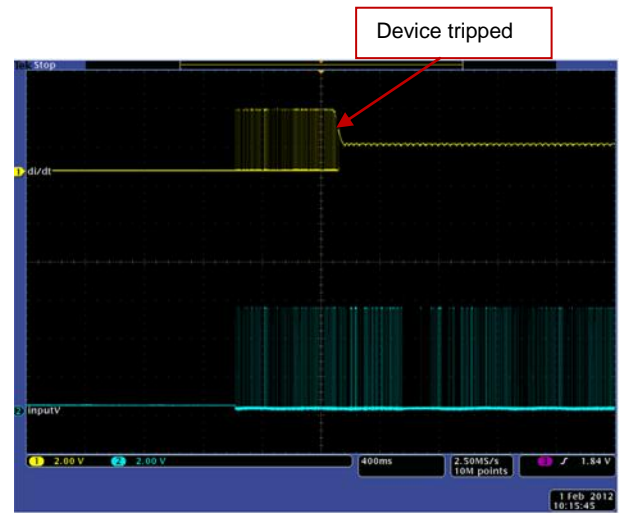


Fig. 11. Function generator output and AFD output screenshot.

By bypassing some of the frontend electronics the power source for the replayed signal can also be much smaller

because the AFD has a step down transformer attached to the PV DC conductor. Thus, the current required to replay the signal can be decreased from PV string levels (~2-15 A) to the milliamp range. However, it is best to test the entire prototype when possible in order to evaluate the performance of the entire detector. Recognizing this, Sensata Technologies is currently building a 10 A arc-fault signature replaying testbed for testing larger systems.

#### IV. CONCLUSIONS

Using an arbitrary function generator, prerecorded baseline and arc-fault waveforms can be consistently regenerated to tune arc-fault detector (AFD) hardware and software systems. This method helped accelerate Sensata Technologies' PV AFD development by eliminating the need for field testing, arc-generating hardware, and data acquisition systems. Further, more scenarios were tested without the need to reconfigure the PV system or locate different PV system components. As a result, robust algorithms were determined, and hardware selection and software algorithm tuning time were greatly reduced. Sensata Technologies employed this technique to accelerate the development of their alpha prototype arc-fault detectors.

#### ACKNOWLEDGEMENT

Sandia National Laboratories is a multi-program laboratory managed and operated by Sandia Corporation, a wholly owned subsidiary of Lockheed Martin Corporation, for the U.S. Department of Energy's National Nuclear Security Administration under contract DE-AC04-94AL85000. Part of this work was funded by the US Department of Energy Solar Energy Technologies Program.

#### REFERENCES

- [1] National Electrical Code, 2011 Edition, NFPA70, National Fire Protection Association, Batterymarch, MA.
- [2] Underwriters Laboratories (UL) Subject 1699B, Outline of Investigation for Photovoltaic (PV) DC Arc-Fault Circuit Protection, April 29, 2011.
- [3] J. Johnson, B. Pahl, C.J. Luebke, T. Pier, T. Miller, J. Strauch, S. Kuszmaul and W. Bower, "Photovoltaic DC arc fault detector testing at Sandia National Laboratories," 37th Photovoltaic Specialists Conference, Seattle, WA, 19-24 June 2011.
- [4] J. Johnson, et al., "Differentiating Series and Parallel Photovoltaic Arc-Faults," 38th Photovoltaic Specialists Conference, Austin, TX, 3-8 June, 2012.
- [5] J. Johnson, et al., "Crosstalk Nuisance Trip Testing of Photovoltaic DC Arc-Fault Detectors," 38th Photovoltaic Specialists Conference, Austin, TX, 3-8 June, 2012.